

Peptide-guided adaptor-CAR T-Cell therapy for the treatment of SSTR2-expressing neuroendocrine tumors

Christian Pellegrino^a, Nicholas Favalli^b, Laura Volta^a, Ramon Benz^a, Sara Puglioli^b, Gabriele Bassi^b, Kathrin Zitzmann^c, Christoph Josef Auernhammer^c, Svenja Nölting^d, Chiara F. Magnani^a, Dario Neri^b, Felix Beuschlein^{d,e,f}, and Markus G. Manz^a

^aDepartment of Medical Oncology and Hematology, University Hospital Zürich (USZ) and University of Zürich (UZH), Comprehensive Cancer Center, Zürich, Switzerland; ^bDepartment of Chemistry, Philochem AG, Otelfingen, Switzerland; ^cDepartment of Medicine II, University-Hospital Munich-Grosshadern, University of Munich, Munich, Germany; ^dDepartment of Endocrinology, Diabetology and Clinical Nutrition, University Hospital Zürich (USZ), University of Zürich (UZH), Zürich, Switzerland; ^eDepartment of Internal Medicine IV and Interdisciplinary Center of Neuroendocrine Tumors of the GastroEnteroPancreatic System (GEPNET-KUM), Ludwig Maximilian University, LMU Klinikum, Munich, Germany; ^fThe LOOP Zurich - Medical Research Center, Zürich, Switzerland

ABSTRACT

Somatostatin receptor type 2 (SSTR2) is one of the five subtypes of somatostatin receptors and is overexpressed on the surface of most gastro-entero-pancreatic neuroendocrine tumors (GEP-NETs), pituitary tumors, paraganglioma, and meningioma, as well as hepatocellular carcinoma and breast cancer. Chimeric antigen receptor (CAR) T-cells are genetically engineered to express an artificial, T-cell activating binder, leading upon ligation to biocidal activity against target-antigen expressing cells. Adaptor-CAR T-cells recognize, via the CAR, a tag on an antigen-binding molecule, building an activating bridge between the CAR and the target cell. We hypothesized that a novel fluorescent-peptide antagonist of SSTR2, called Octo-Fluo, in combination with anti-FITC adaptor CAR (AdFITC(E2)-CAR) T-cells, may function as an on-off tunable activating bridge between the CAR and SSTR2 expressing target cells. In vitro studies confirmed the binding of Octo-Fluo to Bon1-SSTR2 mCherry-Luc cells without evidence of internalization. AdFITC(E2)-CAR T-cells were activated and efficiently induced Bon1-SSTR2 cell death in vitro, in an Octo-Fluo concentration-dependent manner. Similarly, AdFITC(E2)-CAR T-cells in combination with Octo-Fluo efficiently infiltrated the tumor and eliminated Bon1-SSTR2 tumors in immunodeficient mice in therapeutic settings. Both, AdFITC(E2)-CAR T-cell tumor infiltration and biocidal activity were Octo-Fluo concentration-dependent, with high doses of Octo-Fluo, saturating both the CAR and the SSTR2 antigen independently, leading to the loss of tumor infiltration and biocidal activity due to the loss of bridge formation. Our findings demonstrate the potential of using AdFITC(E2)-CAR T-cells with Octo-Fluo as a versatile, on-off tunable bispecific adaptor for targeted CAR T-cell immunotherapy against SSTR2-positive NETs.

ARTICLE HISTORY

Received 31 January 2024
Revised 28 September 2024
Accepted 30 September 2024

KEYWORDS

Adaptor-CAR T-cell;
neuroendocrine tumors;
Octo-fluo bispecific adaptor;
SSTR2



Introduction


Neuroendocrine tumors (NETs) are neoplasms arising from cells of the endocrine and nervous systems. In the United States, the age-adjusted incidence rate increased 6.4-fold from 1973 (1.09 per 100'000) to 2012 (6.98 per 100'000).¹ Currently, there are about 12'000 new cases diagnosed each year and 171'000 patients living with Neuroendocrine tumors (cancer.net) which now represent the second most prevalent malignancy of the gastro-entero-pancreatic (GEP) tract. The current treatment options for advanced-stage NETs are limited and clinical outcomes are poor. Thus, novel therapeutic approaches are required.

Somatostatin receptors (SSTRs) are a family of G protein-coupled receptors that are expressed on the surface of various cells, including those of the endocrine and nervous systems.^{2,3} SSTR2 is one of the five subtypes of somatostatin receptor and is known to be overexpressed on the surface of GEP-NETs,

pituitary adenomas, paraganglioma, and meningioma, as well as hepatocellular carcinoma and breast cancer.^{4,5} Therefore, SSTR2 is a promising target for the development of therapies in NETs. Current targeting tools against SSTR2 are being employed for both diagnostic and therapeutic applications. DOTA-Tyr³-octreotate (DOTA-TATE) is a cyclic peptide agonist, which binds with a high affinity to SSTR2 and SSTR5. Accordingly, specific labeling with either diagnostic or therapeutic isotopes has been explored. [⁶⁸Ga]Ga-DOTA-TATE has been used for the detection of SSTR2-positive tumors such as GEP-NETs and meningioma. In addition, the application of local irradiation with [¹⁷⁷Lu]Lu-DOTA-TATE has shown high specificity and efficacy in slowing the progression of NETs in clinical trials.^{6,7}

Several immunological tools have been assessed against NETs using SSTR2 as tumor-associated antigen (TAA). Si and coworkers developed a novel antibody-drug conjugate

CONTACT Markus G. Manz  markus.manz@usz.ch  Department of Medical Oncology and Hematology, University Hospital Zürich (USZ) and University of Zürich (UZH), Comprehensive Cancer Center, Rämistrasse 100, Zürich, Switzerland

 Supplemental data for this article can be accessed online at <https://doi.org/10.1080/2162402X.2024.2412371>

© 2024 The Author(s). Published with license by Taylor & Francis Group, LLC.

This is an Open Access article distributed under the terms of the Creative Commons Attribution-NonCommercial License (<http://creativecommons.org/licenses/by-nc/4.0/>), which permits unrestricted non-commercial use, distribution, and reproduction in any medium, provided the original work is properly cited. The terms on which this article has been published allow the posting of the Accepted Manuscript in a repository by the author(s) or with their consent.

(ADC), consisting of a mAb IgG1 fused via a chemical linker to monomethyl auristatin E (MMAE).⁸ Using this agent in a clinical study, they demonstrated significant tumor growth retardation. Lee and colleagues developed an anti-SSTR2 × anti-CD3 bispecific antibody including a full Fc domain to extend the serum half-life.⁹ The bispecific antibody displayed potent anti-tumor activity in subcutaneous NSG *in vivo* models. Furthermore, the bispecific antibody was shown to activate CD4 and CD8 T-cells in cynomolgus monkeys.

Another immunotherapeutic option against SSTR2-positive NETs might be chimeric antigen receptor T-cells (CAR T-cells). CAR T-cells are T-cells expressing, via genetic introduction, a synthetic T-cell activating receptor (frequently derived from an antibody) against defined antigens. The approved application of CAR T-cells is currently limited to B-cell and plasma-cell malignancies, targeting CD19 and B-cell maturation antigen (BCMA)^{10, 11, 12} In a recent preclinical study led by Mandriani *et al.*, the authors tested the efficacy of anti-SSTR CAR T-cells against NETs cell lines.¹³ The construct employed two octreotide peptides as SSTR binding moieties, conveying the ability to bind to multiple members of the SSTR family (SSTR2 and SSTR5), and they demonstrated tumor growth retardation in subcutaneous NET xenograft mouse models.

While CAR T-cells show high efficacy in certain settings, it is also becoming evident that they can induce severe side effects such as cytokine release syndrome (CRS), making it desirable to develop on-off regulation of CAR T-cell activity. Several suicide gene mechanisms have been developed to eradicate the CAR T-cells in case of severe adverse events, which, however, results in terminal CAR T-cell loss.^{14, 15} The need for functional on-off regulation of CAR T-cells has led to the development of adaptor-CAR T-cells (Ad-CAR T-Cells)^{16, 17–20} In this setting, Ad-CAR T-cells bind to a tag, which is placed on the TAA binding agent, composed of an antibody construct or a small-molecule ligand. By doing so, the interaction between the Ad-CAR T-cells and the tumor cells depends on the bispecific adaptor's presence.

We here generated and validated a new fluorescent-peptide antagonist of SSTR2, termed Octo-Fluo, and tested this as an adaptor in combination with anti-FITC adaptor-CAR (AdFITC(E2)-CAR) T-cells. We demonstrate the efficient elimination of SSTR2-expressing NET-cells *in vitro* and *in vivo* in therapeutic settings in xenogeneic mouse models.

Results

Octo-Fluo production and surface-binding validation on Bon1-SSTR2 mCherry-Luc cells

We aimed to generate a peptide molecule targeting SSTR2, which would work as a bispecific engager of an anti-FITC Adaptor CAR T-cell platform for the treatment of neuroendocrine tumors (NETs). The SSTR2-binding compound 3, referred to as Octo-Fluo, was obtained through a one-pot procedure, which is described in Figure 1A and detailed in Supp. scheme 1–3. Initially, compound 1 (linker) and fluorescein isothiocyanate were coupled, followed by quenching of the unreacted FITC. The portable SSTR2 antagonist Octo-azido

moiety (Octo-N₃) was then added to the dibenzocyclooctyne group (DBCO) via copper-free alkyne-azide cycloaddition (CuAAC) “click” reaction. This strategy enabled the construction of an SSTR2 receptor-binding fragment connected to fluorescein moiety using a hydrophilic linker, soluble in water at physiological pH. Supplementary Fig. S1–7 shows the HPLC and LC-MS profiles of each reaction step. We then performed titration assays by flow cytometry to assess the binding affinity of the Octo-Fluo to a Bon1-SSTR2 mCherry-Luc cell line, illustrated as histograms in Figure 1b and as a sigmoid curve in Figure 1c. The results confirmed the binding of the Octo-Fluo bispecific adaptor, exhibiting a high affinity toward SSTR2. The immunofluorescence staining of healthy pancreas shown in Figure 1d was performed using the Octo-Fluo as the primary stain, highlighting the specific binding of the Octo-Fluo to SSTR2 expressed on pancreatic islets. Furthermore, using the same staining protocol, we labeled SSTR2 expressing paraganglioma biopsies (Figure 1d). To validate surface binding, we visualized the linker by confocal microscopy studies (Figure 1e). The Octo-Fluo, indicated in green, demonstrated extracellular membrane coating when bound to SSTR2, as well as no accumulation when SSTR2 was absent, as shown with Bon1-WT cells. The mCherry stain, depicted in red, was included as an internal control for an intracellular signal. To confirm the non-internalizing binding of our adaptor molecule when binding SSTR2, we conducted longer adaptor exposure to the Bon1-SSTR2 mCherry-Luc cells at time points of 3 and 6 h at 37°C (shown in Supp. Fig. S8). The results show that at both time points the fluorescein coats the plasma membrane without accumulating intracellularly. Taken together, these findings confirm that the interaction between the Octo-Fluo bispecific adaptor and the Bon1-SSTR2 mCherry-Luc cells results in co-localization and accumulation of the plasma membrane with undetectable internalization in the applied assay.

Production of AdFITC(E2)-CAR T-cells and *in vitro* biocidal activity against Bon1-SSTR2 cells and H69 non-small cell lung cancer cells in combination with Octo-Fluo

Given the promising binding properties of Octo-Fluo, we produced anti-FITC Adaptor CAR T-cells, using a previously published anti-FITC single-chain fragment variable (scFv) generated from the sequence of the E2 antibody.²¹ We generated a lentiviral vector that contains the transgene encoding the AdFITC(E2)-CAR cassette. The second-generation AdFITC(E2)-CAR was linked to RQR8, a marker for gene expression, that may be used for CAR T-cell selection and depletion,¹⁴ via a T2A cleavable linker. The graphical representation depicted in Figure 1f illustrates the various components of the immunotherapeutic system based on AdFITC(E2)-CAR T-cells and the Octo-Fluo bispecific adaptor, acting as a bridging element between effector and SSTR2-expressing target cell. The AdFITC(E2)-CARs were expressed on primary healthy-donor derived T cells (Supp. Fig. 9A). The cytotoxicity assay consisted of co-incubated AdFITC(E2)-CAR T-cells and Bon1-SSTR2 with Octo-Fluo concentrations varying from 30 fM to 3 μM. Target cell death was measured by flow cytometry at 24, 48 and 72 h (Figure 2a–c), highlighting an optimal range of

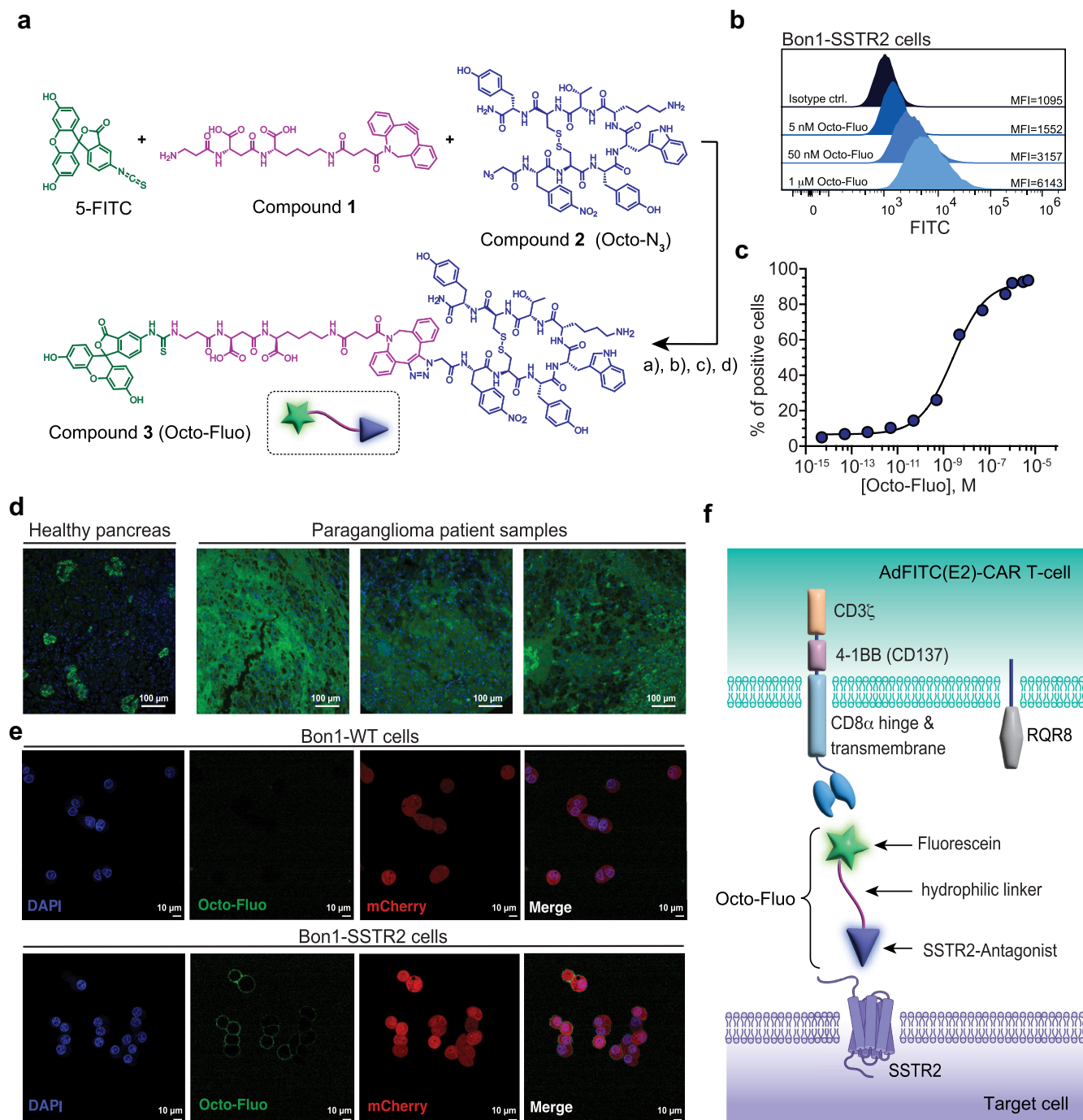


Figure 1. Octo-Fluo synthesis and *in vitro* validation in combination with AdFITC(E2)-car T-cells. (a) Chemical structure and one-pot synthesis of compound 3 (Octo-Fluo). Reaction conditions a) DMSO, TEA (10 eq.), 1 h, 37°C; b) 1-(2-Aminoethyl)piperidine (10 eq.), 15', 37°C; c) DMSO, 15', 37°C; d) formic acid (up to pH ~ 3), HPLC purification. (b, c) Octo-Fluo titration on Bon1-SSTR2 mCherry Luc cell line, analyzed by flow cytometry, shown as a histogram with relative MFI ($n = 3$) (b) and as sigmoid curve (c). (d) Immunofluorescence on healthy pancreas tissue and three Paraganglioma patient samples was performed using the Octo-Fluo adaptor (scale indicates 100 μ m). The green color (fluorescein) and blue (DAPI) represent SSTR2 expression and cell nuclei, respectively. (e) Confocal microscopy pictures after exposure to the Octo-Fluo on Bon1-WT and Bon1-SSTR2 expressing cells. The colors represent the following: Green = Octo-Fluo, Red = mCherry (intracellular), Blue = DAPI (nuclear stain), and the scale bar = 10 μ m. (f) Graphical representation of Octo-Fluo-dependent bridging of AdFITC(E2)-CAR T-cell to the SSTR2-expressing target cell.

concentrations between 0.25 nM and 3 μ M where the highest Bon1-SSTR2 depletion occurred. Furthermore, when validating the cytotoxicity on Bon1-SSTR2-Low and - High cells (Supp. Fig. S11), we show reduced cytolysis at 48 h in the cell lines with a lower SSTR2 expression. However, considering the SSTR2 expression profile of the Bon1-SSTR2-Low cells, the cytolysis at the optimal concentrations of the adaptor is still roughly 40%. To confirm the impact of SSTR2 expression on

lytic activity, we evaluated the system against another cell line, the non-small cell lung cancer cell line H69. H69 expresses low levels of SSTR2, as shown in Supp. Fig. 16 by flow cytometry (Supp. Fig. S16A) and immunohistochemistry (IHC, Supp. Fig. S16B). In similar *in vitro* experiments, as with Bon1-SSTR2+ cells (Figure 2), we observed efficient Octo-Fluo dose-dependent CAR T-cell lytic activity and activation (Supp. Fig. S17).

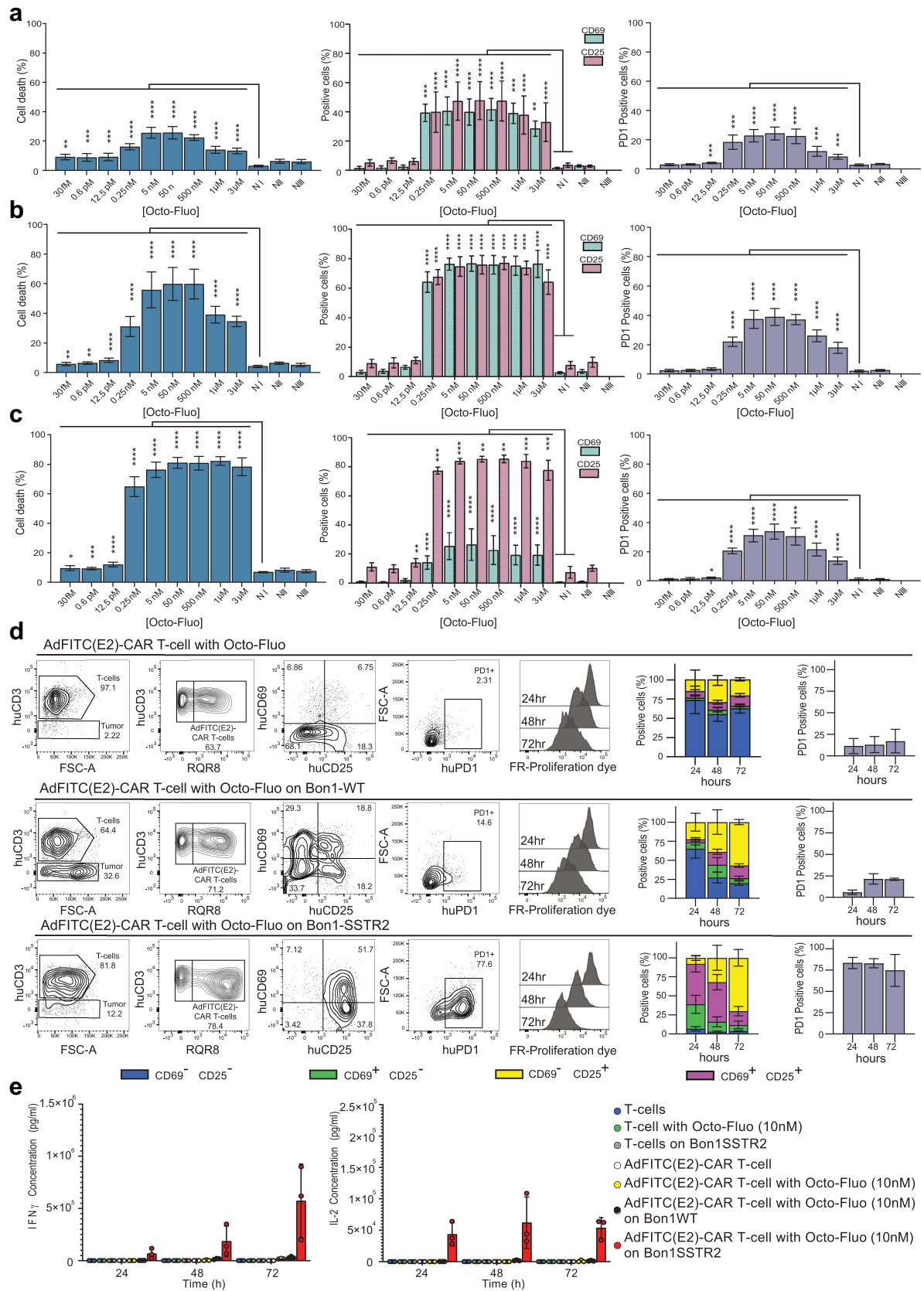


Figure 2. AdFITC(E2)-car T-cells are fully activated *in vitro* only in the presence of both, antigen-expressing target cells and Octo-Fluo adaptor. Quantification of the AdFITC(E2)-CAR T-cell biocidal activity, CD25, CD69 and PD1 expression toward Bon1-SSTR2 mCherry-Luc cells in the presence of increasing concentrations of Octo-Fluo at the indicated time-points 24 h (a), 48 h (b), and 72 h (c) ($n = 3$ donors in triplicate). The effector-to-target ratio was fixed at 1:1. The negative controls to all experiments were as follows: NI; AdFITC(E2)-CAR T-cell with 5 nM Octo-Fluo against Bon1-WT mCherry-Luc cells, NII; AdFITC(E2)-CAR T-cells on Bon1-SSTR2 mCherry-Luc without Octo-Fluo added, NIII; Bon1-SSTR2 with 3 μ M Octo-Fluo. For the statistical analysis, we compared the cell death of each condition to NI. (d) Representative flow cytometry plots illustrating AdFITC(E2)-CAR T-cell activation as determined by CD25, CD69 and PD1 expression as well as by cell division ($n = 3$ donors in triplicate). Effector cells were co-cultured with tumor cells which were SSTR2 negative or positive, in the presence and absence of the Octo-Fluo and analyzed after 48 hr. The

In summary, the biocidal activity of the AdFITC(E2)-CAR T-cells is dependent on the presence of an adequate concentration of the Octo-Fluo bispecific adaptor, with high activity across a 4-log fold concentration range.

AdFITC(E2)-CAR T-cell *in vitro* and *in vivo* activation is conditional to the presence of both the Octo-Fluo adaptor and tumor-associated antigen-expressing cells

We next aimed to determine if the adaptor in the absence of the tumor-target antigen would activate AdFITC (E2)-CAR T-cells, posing a possible safety concern. We ascertained T-cell and AdFITC(E2)-CAR T-cell activation status, assessed by early and late activation markers CD69 and CD25, in the presence and absence of the Octo-Fluo adaptor with or without SSTR2-expressing target cells by respective co-incubation assays. **Figure 2d** illustrates the gating strategy and data acquired by flow cytometry after 48 h of exposure to each condition. AdFITC (E2)-CAR T-cells and control T-cells (Supp. Fig 10) were not activated with the Octo-Fluo alone, as indicated by low or absent CD69/CD25 and PD1 expression. In contrast, when the AdFITC(E2)-CAR T-cells were exposed to Bon1-SSTR2 cells and Octo-Fluo (**Figure 2d**), CD69/CD25 and PD1 expression increased to 58%/89.5% and 77%, respectively. Meanwhile, when we exposed AdFITC(E2)-CAR T-cells to SSTR2 negative tumor cells (Bon1-WT) and Octo-Fluo, CD69/CD25 and PD1 expression increased to 48/37% and 15.4%, respectively. We also assessed the activation status *in vivo*. As shown in Supp. Fig. 12A, we subcutaneously (s.c.) implanted 8×10^6 Bon1-SSTR2 mCherry-Luc tumor cells in the flank of NSG mice. After 14 d, once the tumors reached an average size of 80 mm^3 , mice were treated by intravenous (i.v.) administration of 10^7 AdFITC(E2)-CAR T-cells, with or without concomitant i.v. injection of Octo-Fluo (0.5 nmol every 12 h). On day 21, upon terminal analysis, we harvested blood, spleen and tumor and analyzed them via flow cytometry. The AdFITC (E2)-CAR T-cell activation status in the spleen underlined a comparable inactive state between mice receiving AdFITC(E2)-CAR T-cells alone and with the adaptor (Supp. Fig. 12B). However, in the tumor tissues (Supp. Fig. 12B), the AdFITC(E2)-CAR T-cells alone were not detected (ND), whereas the group that received the adaptor demonstrated tumor infiltration, with a marked polarization toward CD69+CD25- and CD69+CD25+ active state. The intra-tumor AdFITC(E2)-CAR T-cells seem to be shifted toward CD8 cytotoxic T-cells, as shown in Supp. Fig. 12D, when compared to the CD4:CD8 ratios observed in the spleen of the same animals. To test if phenotypic T-cell activation correlated with cytokine release, we measured IL-2 and IFN γ in supernatants of co-cultures in each condition (**Figure 2e**). The results demonstrate strong cytokine release only in the presence of all elements, AdFITC(E2)-CAR T-cells, Octo-Fluo and Bon1-SSTR2. Supp. Fig. 12E describes

the model used to validate the on-demand AdFITC(E2)-CAR T-cell activity by measuring IFN γ release detected from the serum. The schematic representation delineates that on day 17 we halted the infusions of the adaptor molecule, whilst maintaining the administrations in the positive control group. On day 21, we terminated the experiment and collected the serum. The IFN γ levels at day 17 show that the group that received both the AdFITC(E2)-CAR T-cell and the adaptor yielded significantly higher IFN γ levels when compared to AdFITC(E2)-CAR T-cells alone. On day 21, the group that continued to receive the adaptor infusions showed a significant increase in IFN γ secretion compared to the group where the adaptor injections were stopped. Thus, these data indicate that binding of Octo-Fluo to AdFITC (E2)-CAR T-cells without crosslinking to SSTR2-expressing target cells will likely not cause a safety limitation of the approach.

Tumor eradication by AdFITC(E2)-car T-cells *in vivo*

To determine the efficacy of AdFITC(E2)-CAR T-cells in combination with Octo-Fluo *in vivo*, we subcutaneously (s.c.) implanted 8×10^6 Bon1-SSTR2 mCherry-Luc tumor cells in the flank of NSG mice. After 14 d, once the tumors reached an average size of 80 mm^3 , mice were treated by intravenous (i. v.) administration of 10^7 AdFITC(E2)-CAR T-cells, with or without concomitant i.v. injection of Octo-Fluo (2.5 or 0.5 nmol every 12 h). The experimental setup is shown in **Figure 3a**. In mice receiving PBS and only AdFITC (E2)-CAR T-cells, the tumors grew in similar kinetic and size, whereas tumors were eradicated by twice daily additional application of Octo-Fluo (**Figure 3b–d**). The quantification of the total flux illustrated in **Figure 3c** underlines the slower tumor eradication kinetics of the 2.5 nmol Octo-Fluo group compared to the reduced dose group of 0.5 nmol. The tumor volume and body weight changes, shown in **Figure 3d**, highlight the maintenance of health in the groups that received 0.5 and 2.5 nmol of Octo-Fluo, whereas the control groups showed a decrease in body weight, likely due to tumor progression. To investigate if these findings would also be observed with a cell line expressing lower antigen levels, we subcutaneously implanted 5×10^6 H69 tumor cells in the flanks of NSG mice (see Supp. Fig. S18A). At day 18, when tumors averaged 80 mm^3 in size, mice received an intravenous administration of 10^7 AdFITC(E2)-CAR T-cells, with or without simultaneous intravenous injections of Octo-Fluo (0.5 nmol every 12 h). Mice treated with PBS, the Octo-Fluo adaptor alone, or AdFITC(E2)-CAR T-cells alone exhibited rapid tumor growth. In contrast, mice treated with both AdFITC(E2)-CAR T-cells and the Octo-Fluo adaptor showed delayed tumor progression (Supp. Fig. S18B). Analysis of tumors by IHC revealed low infiltrates of huCD3+ and huCD25+ AdFITC(E2)-CAR T-cells in the Octo-Fluo treatment group, while mice that received only AdFITC(E2)-CAR T-cells showed no CAR T-cell infiltration (Supp. Fig. S18C).

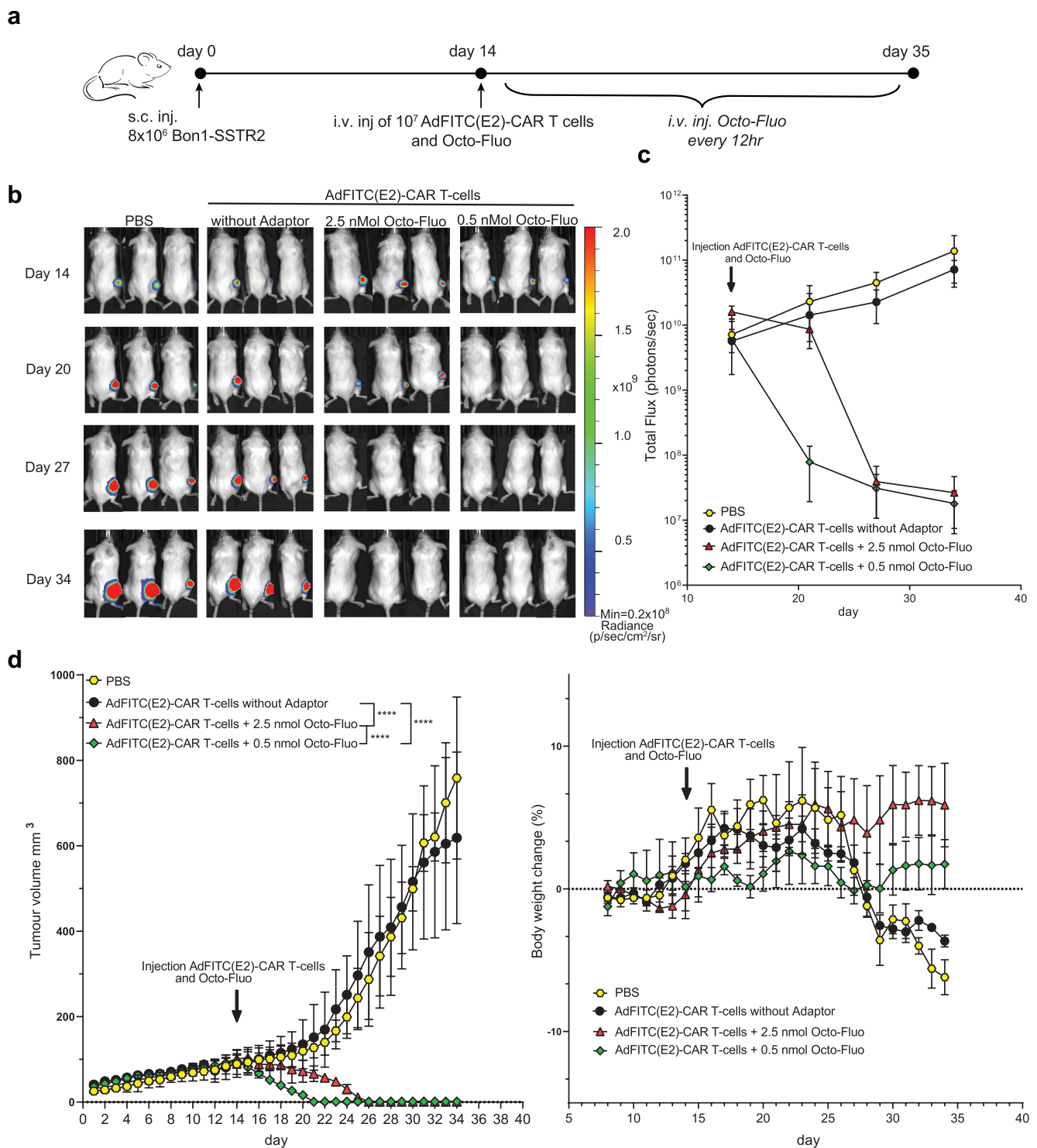


Figure 3. AdFITC(E2)-car T-cells in combination with Octo-Fluo eliminate established Bon1-SSTR2 mCherry-luc tumors *in vivo*. (a) Schematic representation of the *in vivo* therapy set-up. At day 0, NSG mice were injected s.c. in the flank with 8×10^6 Bon1-SSTR2 mCherry-Luc positive cells. Tumors reached ± 0 mm³ on day 14 and were detectable by bioluminescence (IVIS); mice subsequently received 10^7 AdFITC(E2)-CAR T-cells i.v. and either none or 2.5 nmol or 0.5 nmol of Octo-Fluo every 12 h i.v. for 3 weeks; mice were sacrificed at day 35 ($n = 3$ mice per group). (b) Bioluminescence imaging of mice before treatment and at the indicated time points. (c) Graphical quantification of the total IVIS flux measured in the analysis shown in B. (d) Tumor volume and mouse body weight change during the experiment. For the statistical analysis, not shown = not significant, **** $p \leq 0.0001$ (two-way ANOVA test, followed by Bonferroni's multiple comparison test).

Together, the results indicate a strong *in vivo* anti-tumor response in highly SSTR2-expressing Bon1 tumors and a delayed tumor progression in lower SSTR2-expressing H69 tumors, correlated with a higher and lower CAR T-cell infiltration.

Excess administration of Octo-Fluo *in vivo* inhibits AdFITC(E2)-car T-cell tumor infiltration and function

To further assess the Octo-Fluo dose-dependent effect, we repeated the experiment with the working doses of 0.5, 2.5 and a higher dose of 12.5 nmol. Figure 4a summarizes the

experimental setup. Briefly, 8×10^6 Bon1-SSTR2 mCherry-Luc tumor cells were engrafted s.c. in the flank of NSG mice. After 14 d, mice were administered i.v. 10^7 AdFITC(E2)-CAR T-cells. For this experiment, we i.v.-injected every 12 h with three increasing doses of Octo-Fluo: 0.5, 2.5, and 12.5 nmol. As shown by Supp. Fig. 13, tumor volume measurements indicate that twice daily injection of 12.5 nmol of Octo-Fluo hindered the anti-tumor response by saturating both the AdFITC(E2)-CARs and SSTR2 present on the tumor cell. Overall, we did not observe significant toxicities between the treatment arms, as shown by the body weight in Supp. Fig. 13C. Furthermore, as confirmed also by the experiment described in Supp. Fig. 14,

the antagonist alone does not induce tumor growth retardation. This resulted in tumor outgrowth, while 2.5 and 0.5 nmol both exhibited tumor responses. To further understand the mechanism behind these different outcomes, we analyzed the distribution of the AdFITC(E2)-CAR T-cells in blood, spleen and tumors, as shown in Figure 4b. The findings illustrate that regular injections of 12.5 nmol Octo-Fluo resulted in the absence of AdFITC(E2)-CAR T-cells in the tumor microenvironment, which instead remained present in the blood and spleen, albeit showing a significant expansion when compared to the AdFITC(E2)-CAR T-cells without Octo-Fluo injection. To better understand whether the expansion we see in the 12.5

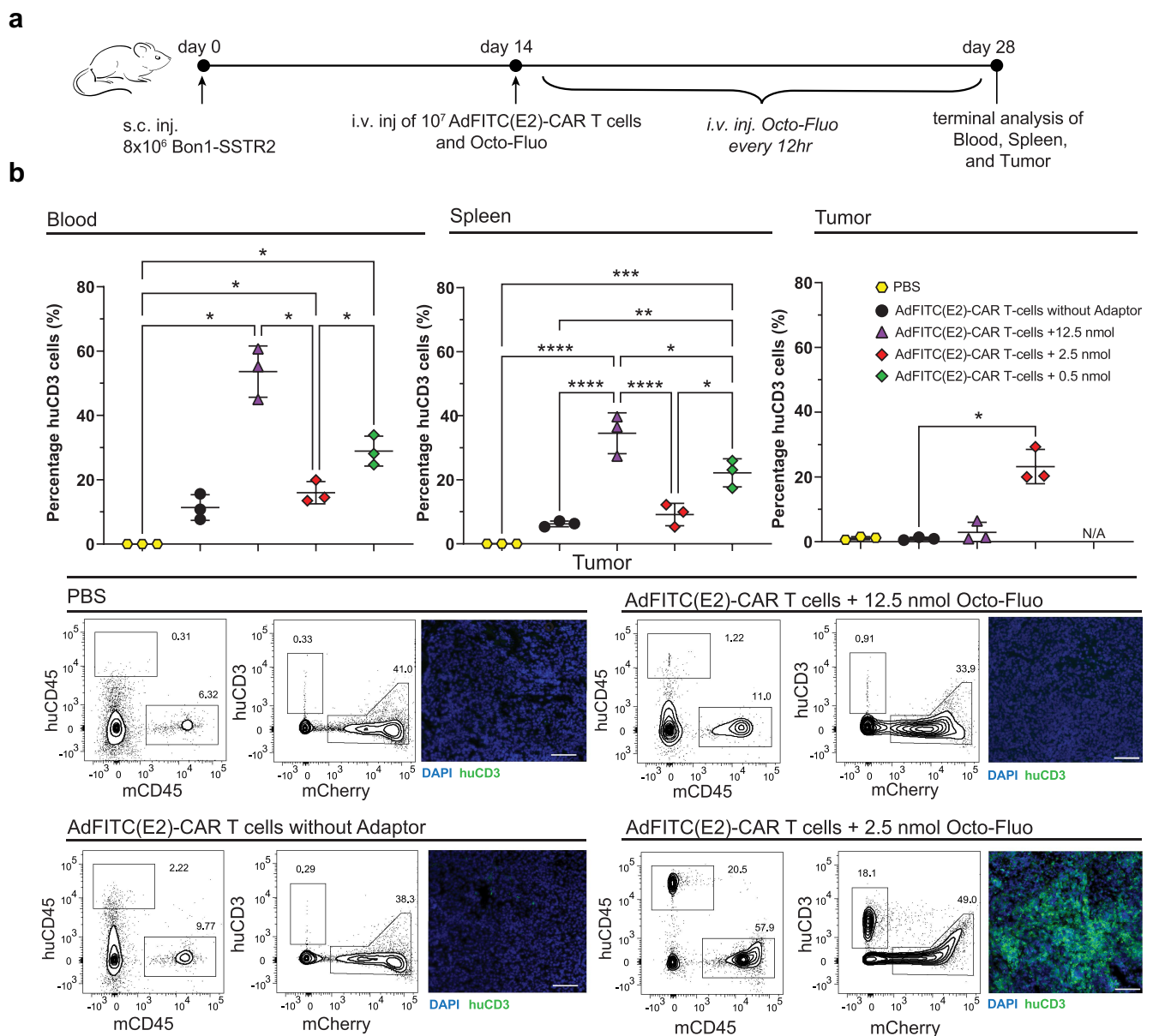


Figure 4. Octo-Fluo dose-dependent *in vivo* anti-tumor efficacy of AdFITC(E2)-car T-cells. (a) Schematic representation of the dose escalation study. On day 0, NSG mice were injected s.c. in the flank with 8×10^6 Bon1-SSTR2 mCherry-Luc positive cells. On day 14 (at a tumor volume of ± 0 mm³), 10^7 AdFITC(E2)-CAR T-cells were injected i.v. followed by either 12.5 nmol, 2.5 nmol, or 0.5 nmol Octo-Fluo i.v. injections repeatedly every 12 h. PBS-injected mice and AdFITC(E2)-CAR T-cell (without Octo-Fluo) injected mice served as negative control. Mice (blood, spleen and tumor) were terminally analyzed at day 28 ($n = 3$ mice per group). For the statistical analysis, not shown = not significant, **** $p \leq 0.0001$, *** $p \leq 0.0002$, ** $p \leq 0.003$, * $p \leq 0.01$ (two-way ANOVA test, followed by Turkey's multiple comparison test) (b) Percentage of AdFITC(E2)-CAR T-cells detected by flow cytometry (huCD45⁺, and huCD3) in blood, spleen and tumor tissues of mice at day 28. The mice treated with both AdFITC(E2)-CAR T-cells and 0.5 nmol Octo-Fluo achieved complete tumor eradication. Therefore, quantification of huCD3-positive tumor-infiltrating cells was not possible. (c) Flow cytometry and immunofluorescence (huCD3) data showing the human immune cell infiltration in tumors at day 28 (scale indicates 100 μ m).

nmol group in Figure 4b is antigen-mediated, Supp. Fig. 15 describes an *in vivo* therapy study in mice implanted with Bon1-WT tumors (SSTR2 negative). The results, shown in Supp. Fig. 15B underlines no relevant expansion in blood, spleen and tumor tissues when comparing mice that received AdFITC(E2)-CAR T-cells with or without the adaptor molecule. Meanwhile, when mice were treated with 2.5 nmol of Octo-Fluo (Figure 4b), there was a marked increase in AdFITC(E2)-CAR T-cells in the tumor mass, while only a low population density was observed in the blood and spleen. Further, the AdFITC(E2)-CAR T-cell distribution in mice treated with 0.5 nmol Octo-Fluo indicated that once the tumor was eradicated, the AdFITC (E2)-CAR T-cells remained mainly present in the blood and spleen. Figure 4b depicts flow cytometry plots and immuno-fluorescence staining of tumors. Together, these data suggest that the dose of the bispecific adaptor Octo-Fluo impacts the ability of the AdFITC(E2)-CAR T-cell to infiltrate and ultimately support a tumor response.

Discussion

In this study, we present a novel peptide bispecific adaptor targeting SSTR2, an antigen broadly expressed in neuroendocrine tumors. Moreover, we provide pre-clinical *in vitro* and *in vivo* evidence of the anti-tumor efficacy of a tunable adaptor CAR T cell platform against an SSTR2-positive pancreatic neuroendocrine tumor model. This technology may facilitate the translation of a safe and effective strategy in a category of patients associated with poor outcomes.

One of the major hurdles for cell-surface molecule targeting immunotherapies in oncology is tumor-cell specificity. Currently approved, efficient immunotherapies do not sufficiently discriminate between healthy cell-of-origin tissue and malignant cells. Clinically approved CAR T cells that target highly B- and plasma-cell lineage-specific markers, such as CD19 and BCMA in B- and plasma cell malignancies, ablate healthy B- and plasma cells, leading to B-cell aplasia and hypogammaglobulinemia. A similar approach of tissue-specific antigen targeting in solid tumors would lead to organ ablation and would only be clinically acceptable if the respective organ is not vital.

SSTR family proteins have been employed as TAAs to image primary and metastatic NETs, small-cell lung cancers, and meningiomas using the radiolabeled peptide DOTA-TATE.^{22,23} Notably, [⁶⁸Ga]Ga-DOTA-TATE demonstrated only affinity to SSTR2 and selective accumulation in metastatic lesions of NETs, providing a clean profile for diagnostic and therapeutic purposes.^{24,25} More recently, several reports have identified numerous antagonist somatostatin analogs that visualized SSTR2-positive tumors better than conventional agonists in both preclinical and clinical cases.^{26,27} We evaluated the binding and interaction of Octo-Fluo, a novel fluorescently labeled SSTR2 peptide antagonist, with the Bon1-SSTR2 mCherry-Luc tumor cell line. Titration experiments and confocal microscopy revealed a high-affinity interaction with the decoration of the extracellular membrane of SSTR2-expressing tumor cells. Notably, our data showed that Octo-Fluo interacts with SSTR2-positive cells without inducing SSTR2

internalization, which would not allow adaptor CAR T-cell activity.^{28,29} High affinity for the target in the absence of internalization, together with the high discrimination between SSTR2-expressing paraganglioma patient samples and healthy pancreas, indicates that Octo-Fluo binding properties are suitable for exploitation in a targeting approach aimed to favor high specificity and accessibility to the tumor site.

Increased accessibility of small molecules to the site of action compared to antibody-based strategies may leverage CAR T-cell immunotherapy employing adaptors. There have been numerous studies promoting multiple tag designs for adaptor CAR T-cell therapies^{30, 31,32} In our study, we focused on using fluorescein as a CAR ligand, conjugated to an antigen-targeting small molecule bispecific adaptor. One of the reasons why we chose fluorescein is the current clinical application as a diagnostic dye in ophthalmology or endomicroscopy, where fluorescein is injected intravenously without reported overt safety concerns.³³

Small molecule bispecific adaptors convey several advantages for Adaptor CAR T-cell technology. Due to their small size, the risk of developing an antibody-based antigen response is lower, as their half-life is very short (~30 min), compared to long-lived antibodies^{34, 35,36} which would also ensure a tighter control over the AdFITC-CAR T-cell activity where cessation of administration would rapidly result in CAR T-cell detachment from the target cells. In addition, the material cost of small molecule-based compared to antibody-based bispecific adaptors is substantially reduced, with a 10-fold difference when it comes to GMP-grade production for clinical investigations.³⁷

We observed that the biocidal activity of AdFITC(E2)-CAR T-cells co-cultured *in vitro* with Bon1-SSTR2 mCherry-Luc cells was dependent on the dose of Octo-Fluo bispecific adaptor, indicating that our platform is highly tunable by different amounts of the small molecule bispecific adaptor. Furthermore, the strong cytolytic efficacy toward Bon1-SSTR2-Low expressing cells suggests that the system described in this study is highly antigen-sensitive. These findings align with *in vitro* and *in vivo* experiments on SSTR2-low-expressing H69 non-small cell lung cancer cells. Despite the lower expression, significant tumor growth delay was observed in mice treated with AdFITC(E2)-CAR T-cells and the Octo-Fluo adaptor. The reduced response, compared to Bon1-SSTR2, is likely in part due to a poorer AdFITC(E2)-CAR T-cell infiltration and expansion, leading to an unfavorable effector-to-target ratio within the tumor.

In line with this, not only the AdFITC(E2)-CAR T-cell biocidal activity was modulated but also the cytokine release was diminished when the Octo-Fluo molecule dose was at either end of the optimal dose window. These findings are in line with previous reports, showing that the adaptor CAR T-cell systems can be controlled by the presence and amount of bispecific adaptor.^{16,38–40}

Being a small molecule conjugated with a single fluorescein, the Octo-Fluo is characterized by a monovalent engagement of the AdFITC(E2)-CAR molecule. This contact is similar to the engagement bispecific antibodies achieve as they engage the TCR complex in a monovalent interaction, preventing systemic activation of effector cells in the absence of the target

cells.⁴¹ Our findings are aligned with what had previously been reported by Chang and colleagues when studying monomeric and dimeric interactions with CARs.⁴² Their study suggested that CAR T-cell activation relies on CAR dimerization and that monomeric interactions do not elicit an activation. We show that the exposure of the AdFITC(E2)-CAR T-cell to the Octo-Fluo adaptor without the presence of target antigen does not induce dimerization, hence we do not observe activation by CD69 and CD25 measurements. Moreover, we demonstrate that the AdFITC(E2)-CAR T-cell activation only takes place in the tumor, where SSTR2 is present, and these produce pro-inflammatory cytokines such as IFN γ that can be detected in the serum. Only when both elements are exposed to an SSTR2-expressing cell line, do the tumor cells act as solid support for multiple interactions, leading to dimerization and ultimately AdFITC(E2)-CAR T-cell activation and proliferation.

The *in vivo* experiments investigating the impact of the dose at a fixed injection schedule of Octo-Fluo highlighted the importance of both the activity and the biodistribution of the AdFITC(E2)-CAR T-cells. These findings support previously published studies by Lee *et al.*, where they showed that increasing five-fold the optimal dose led to tumor persistence.³⁸ In our study, we demonstrate that 25-fold the optimal dose resulted in a hindered tumor response compared to the 0.5 nmol and 2.5 nmol of adaptor molecule. When comparing the biodistribution of the mice that received AdFITC(E2)-CAR T-cells alone or in combination with 12.5 nmol of adaptor, we notice a significant increase in the blood and spleen of AdFITC(E2)-CAR T-cells, although the tumor response is comparable to the negative control groups that received PBS or AdFITC(E2)-CAR T-cells without the adaptor. This suggests a possible time-frame where the dose allows antigen-mediated AdFITC(E2)-CAR T-cell expansion. However, not only did the dose quench the AdFITC(E2)-CAR and SSTR2 binding sites but it also restricted AdFITC(E2)-CAR T-cell tumor infiltration and subsequent expansion.

While the use of bispecific adaptors may allow excellent anti-tumor activity combined to control CAR T cell-derived toxicities, a limitation of the proposed approach might be the need for tight tuning of the three elements, which may complicate clinical development. Careful study design of the clinical trial will be needed to find the optimal dose allowing productive recognition. A key aspect to take into consideration is the presence of SSTR2, which is not only found in cancerous lesions but is also present in healthy tissues such as the pancreas, brain, and gastrointestinal tissues.^{43,44} Numerous studies have confirmed the increased expression of SSTR2 in cancers like breast cancer and rectal NETs compared to healthy counterparts.^{45,46} Although the levels are lower in healthy tissues, this highlights the need for caution in future clinical applications and supports the development of systems that rely on adaptors to limit potential severe side effects on healthy tissues. This should also be even more complex when including multiple small molecule binders to target heterogeneous tumors. To ensure safety, the small molecules will likely be tested singularly in combination with AdFITC CAR T-cells and eventually evaluated together in a second step. In this study, we adopted a peptide-based bispecific adaptor with high affinity toward SSTR2 that was able to promote potent

engagement of the effector cells toward the cancer target. To develop this technology further, *de novo* discovery of small molecules and incorporation of alternative bispecific adaptors such as peptide ligands, may allow a broader application to other cancer entities.

Materials and methods

Synthesis of Octo-Fluo

All reactions were carried out in the dark to preserve fluorescein spectrophotometric performance. Fluorescein isothiocyanate isomer 5 (5-FITC) and Compound **1** were dissolved in DMSO, and triethylamine was added. The resulting solution was mixed for 1 h at 37°C, upon full conversion of compound **1**. Compound **1E**, consisting of the FITC conjugated to the linker without the antagonist, was used as an isotype control for the flow cytometry experiments. The excess of 5-FITC was quenched by the addition of 1-(2-Aminoethyl)piperidine and subsequently, a solution of compound **2** in DMSO was added to the reaction. The resulting mixture was stirred at 37°C for 15 min. Upon full conversion of compound **2** to compound **3**, the reaction was quenched with formic acid (to a pH ~ 3) and compound **3** (Octo-Fluo) was isolated by reverse-phase HPLC. For the detailed procedure see the supplementary information (synthesis steps described in detail in Supp. Figure S1-7).

AdFITC(E2)-CAR T-cell generation and storage

Healthy donors' buffy coats were acquired from the Zürich blood donation service (Blutspende Zürich, Zürich, Switzerland). PBMCs were enriched by density gradient centrifugation (Ficoll-Paque Plus, GE healthcare). T-cells were then negatively isolated with EasySepTM beads (Human T cell isolation kit, STEMCELL Technologies). Human T-cells were activated in T-cell medium supplemented with CD3/CD28 Dynabeads (ThermoFisher) the day before transduction.⁴⁷ For the transduction, Polybrene (Santa Cruz Biotechnology, #134220) was added to a final concentration of 8 $\mu\text{g}/\text{mL}$, and 10 μL virus supernatant was added to the cells and mixed. After centrifugation (1000 g, 90 min, 32°C) the cells were incubated overnight (37°C, 5% CO₂). On the following day, the media was exchanged, and the T-cells were incubated overnight (37°C, 5% CO₂). The beads were magnetically removed and resuspended in fresh T-cell medium and expanded at 1×10^6 cells/mL. The AdFITC(E2)-CAR T-cells were expanded until day 10 when they were cryopreserved and stored at -180°C.

In vivo therapeutic studies

All procedures involving experimental animals were performed according to protocols approved by the Cantonal Veterinary Office Zurich (006/2021 and 134/2022). On day 0, NSG mice (NOD.Cg-Prkdcscid Il2rgtm1Wjl/SzJ) were transplanted s.c. with 8×10^6 Bon1-SSTR2 mCherry-Luc cells. Once the tumor volume reached $\pm 80 \text{ mm}^3$, 10^7 AdFITC(E2)-CAR T-cells were injected i.v. followed immediately by an injection i.v. of Octo-Fluo at the indicated amount. The tumor burden

was evaluated weekly by BLI and daily caliper measurements. The Octo-Fluo i.v. injections were repeated every 12 hr until the termination of the experiment.

Immuno-fluorescence

Healthy pancreas and Paraganglioma patient samples were cut (3 μm) and mounted on SuperFrostTM slides (Thermo Fisher Scientific).⁴⁸ The tissues were processed by the Department of Pathology, University Hospital Zurich. For the patient-derived paraganglioma Immuno-Fluorescence staining, slides were subjected to the Octo-Fluo molecule (150 nM) as the primary stain, followed by rabbit anti-FITC antibody (Catalogue number #4510–7804, BioRad), and donkey anti-rabbit Alexa 488 (Catalogue number #A21206, Invitrogen). To visualize the nucleus, we added the mounting medium with DAPI (Abcam) before adding the microscope cover glass (Ref. ECN631–1574). Slides were stained with the Ventana Optiview platform (Ventana Medical Systems) according to the manufacturer's protocols. The images were taken with an upright epifluorescence microscope (DM5500-B, Leica) at 20 \times magnification (HC PL FLUOTAR 5 \times /0.15 Leica objective). Leica LAS-X software was used for microscope control, image acquisition and analyses. All staining intensities were compared to isotype controls.

At the terminal analysis of mice, the tumor tissues were cut in half. One-half of the tumor was processed by flow cytometry as described below, the other was embedded in OCT-medium. The OCT-blocks were then cut into 8 μm slices and mounted on SuperFrostTM Plus slides (Thermo Fisher Scientific). The slides were then permeabilized in an EasyDip slide staining system (Milian) containing ice-cold Acetone. To stain the tissues, we drew a hydrophobic square around the sample using Pap pen (Dako, Catalogue number #S2002). To visualize the CD3⁺ cells, the slides were stained with the anti-CD3d rabbit monoclonal antibody (Cat. Num. MA5–32462 Invitrogen), followed by rabbit anti-FITC antibody (Catalogue number #4510–7804, BioRad), and donkey anti-rabbit Alexa 488 (Catalogue number #A21206, Invitrogen). To visualize the nucleus, we added the mounting medium with DAPI (Abcam) before adding the microscope cover glass (Ref. ECN631–1574). The images were taken with an upright epifluorescence microscope (DM5500-B, Leica) at 20 \times magnification (HC PL FLUOTAR 5 \times /0.15 Leica objective). Leica LAS-X software was used for microscope control, image acquisition and analyses. All staining intensities were compared to isotype controls.

Ex vivo terminal analysis and tissue processing

The homogenized tumor, spleen and blood were treated with Red Blood Cell Lysis Buffer (BioLegend). Once re-suspended in the FACS buffer, all tissue samples were filtered through a 70- μm cell strainer. To discriminate the live cells from the dead, we stained the cells with Zombie Aqua Viability Kit (BioLegend) for 30 min at 4°C. The tissue samples were subsequently stained using anti-huCD45, anti-muCD45, and anti-huCD3 (Biolegend) for 30 min at 4°C. The samples were ultimately strained (30 μm nylon mesh) and analyzed via flow

cytometry (BD LSRFortessaTM cell analyzer, BD biosciences). The flow cytometry data were analyzed using FlowJo software (Treestar).

Acknowledgments

We thank Prof. Dr Martin Ehrbar for the use of the fluorescence Leica microscope. We thank Prof. Dr Patrick Salmon (University of Geneva, Switzerland) for the lentiviral backbones. In addition, we thank Prof. Dr Brian Philip and Prof. Dr Martin Pule for providing the RQR8 sequence used for this study. We thank Susanne Dettwiler and Fabiola Prutek for their help in staining the patient-derived tissues for immuno-fluorescence and immunohistochemistry experiments. We thank Dr Constanze Hantel for the help in sequencing the cell line, and Dr Ana Maria Quintela Pousa for their technical contribution.

Financial support by the Hochschulmedizin Zürich Program "Immuno-targET" to Prof. Dr Dario Neri, Prof. Dr Markus G. Manz, and Prof. Dr Felix Beuschlein, and the Innosuisse Innovation project (55003.1 IP-LS) to Prof. Dr Dario Neri, Prof. Dr Markus G. Manz and Dr Christian Pellegrino is gratefully acknowledged.

Disclosure statement

CP, GB, NF, DN, FB and MGM are inventors of a patent application that describes the Octo-Fluo molecule.

Funding

The work was supported by the Hochschulmedizin Zürich [ImmunoTargET]; Innosuisse – Schweizerische Agentur für Innovationsförderung [120.421 IP-LS].

Author contributions:

NF, SP, GB, DN designed the Octo-Fluo bispecific adaptor. NF and SP synthesized and ran quality control on the Octo-Fluo molecule. KZ, CA, SN worked on the generation and establishment of the Bon1-SSTR2 cell line. CH was involved in the sequencing of the Bon1-SSTR2 cell line. CP, NF performed the validation of the Octo-Fluo by flow cytometry, Immuno-Fluorescence and confocal microscopy validation. CP produced the AdFITC(E2)-CAR T-cells and RB contributed to the in vitro validation. LV designed the mCherry-Luciferase construct and CP produced the lentiviral vector used to transduce the Bon1-SSTR2. CP conducted the in vivo validations and injections and CP and LV performed terminal analysis of mice. CP, NF, MGM, DN, FB, and CM contributed to the writing of the manuscript. FB, DN and MGM directed the studies.

Data availability statement

Raw data were generated at University Hospital Zürich (USZ) and Philochem AG. Derived data supporting the findings of this study are available both in the Supplementary Information and from the corresponding author MGM on request.

References

1. Dasari A, Shen C, Halperin D, Zhao B, Zhou S, Xu Y, Shih T, Yao JC. Trends in the incidence, prevalence, and survival outcomes in patients with neuroendocrine tumors in the United States. *JAMA Oncol.* 2017;3(10):1335. doi:10.1001/jamaoncol.2017.0589.
2. Taniyama Y, Suzuki T, Mikami Y, Moriya T, Satomi S, Sasano H. Systemic distribution of somatostatin receptor subtypes in human: an immunohistochemical study. *Endocr J.* 2005;52(5):605–611. doi:10.1507/endocrj.52.605.

3. Harda K, Szabo Z, Juhasz E, Dezso B, Kiss C, Schally AV, Halmos G. Expression of somatostatin receptor subtypes (SSTR-1–SSTR-5) in pediatric hematological and oncological disorders. *Molecules*. 2020;25(23):5775. doi:10.3390/molecules25235775.
4. Wu W, Zhou Y, Wang Y, Liu L, Lou J, Deng Y, Zhao P, Shao A. Clinical significance of somatostatin receptor (SSTR) 2 in Meningioma. *Front Oncol*. 2020;10:1633. doi:10.3389/fonc.2020.01633.
5. Yin X, Wang P, Yang T, Li G, Teng X, Huang W, Yu H. Identification of key modules and genes associated with breast cancer prognosis using WGCNA and ceRNA network analysis. *Aging Albany NY*. 2020;13(2):2519–2538. doi:10.18632/aging.202285.
6. Strosberg JR, Srirajaskanthan R, El-Haddad G, Wolin EM, Chasen BA, Kulke MH, Bushnell DL, Caplin ME, Baum RP, Hendifar AE. et al. Symptom diaries of patients with midgut neuroendocrine tumors treated with 177Lu-dotatate. *J Nucl Med*. 2021;62(12):1712–1718. doi:10.2967/jnumed.120.258897.
7. Clement D, Navalkisoor S, Srirajaskanthan R, Courbon F, Dierickx L, Eccles A, Lewington V, Mitjavila M, Percovich JC, Lequoy B. Efficacy and safety of 177Lu-dotatate in patients with advanced pancreatic neuroendocrine tumours: data from the NETTER-R international, retrospective study. *Eur J Nucl Med Mol Imag*. 2022;49(10):3529–3537. doi:10.1007/s00259-022-05771-3.
8. Si Y, Kim S, Ou J, Lu Y, Ernst P, Chen K, Whitt J, Carter AM, Markert JM, Bibb JA. Anti-SSTR2 antibody-drug conjugate for neuroendocrine tumor therapy. *Cancer Gene Ther*. 2021;28(7–8):799–812. doi:10.1038/s41417-020-0196-5.
9. Lee S-H, Chu SY, Rashid R, Phung S, Leung IW, Muchhal US, Moore GL, Bernett MJ, Schubert S, Ardila C. et al. Abstract 3633: anti-SSTR2 × anti-CD3 bispecific antibody induces potent killing of human tumor cells in vitro and in mice, and stimulates target-dependent T cell activation in monkeys: a potential immunotherapy for neuroendocrine tumors. *Cancer Res*. 2017;77(13_Supplement):3633–3633. doi:10.1158/1538-7445.AM2017-3633.
10. Maude SL, Laetsch TW, Buechner J, Rives S, Boyer M, Bittencourt H, Bader P, Verneris MR, Stefanski HE, Myers GD. et al. Tisagenlecleumab in children and young adults with B-Cell lymphoblastic leukemia. *N Engl J Med*. 2018;378(5):439–448. doi:10.1056/NEJMoa1709866.
11. Raje N, Berdeja J, Lin Y, Siegel D, Jagannath S, Madduri D, Liedtke M, Rosenblatt J, Maus MV, Turka A. et al. Anti-BCMA CAR T-Cell therapy bb2121 in relapsed or refractory multiple myeloma. *N Engl J Med*. 2019;380(18):1726–1737. doi:10.1056/NEJMoa1817226.
12. Labanieh L, Mackall CL. CAR immune cells: design principles, resistance and the next generation. *Nature*. 2023;614(7949):635–648. doi:10.1038/s41586-023-05707-3.
13. Mandriani B, Pellè E, Mannavola F, Palazzo A, Marsano RM, Ingravallo G, Cazzato G, Ramello MC, Porta C, Strosberg J. et al. Development of anti-somatostatin receptors CAR T cells for treatment of neuroendocrine tumors. *J Immunother Cancer*. 2022;10(6):e004854. doi:10.1136/jitc-2022-004854.
14. Philip B, Kokalaki E, Mekkaoui L, Thomas S, Straathof K, Flutter B, Marin V, Marafioti T, Chakraverty R, Linch D. et al. A highly compact epitope-based marker/suicide gene for easier and safer T-cell therapy. *Blood*. 2014;124(8):1277–1287. doi:10.1182/blood-2014-01-545020.
15. Sahillioglu AC, Schumacher TN. Safety switches for adoptive cell therapy. *Curr Opin Immunol*. 2022;74:190–198. doi:10.1016/j.coi.2021.07.002.
16. Pellegrino C, Favalli N, Sandholzer M, Volta L, Bassi G, Millul J, Cazzamalli S, Matasci M, Villa A, Myburgh R. et al. Impact of ligand size and conjugation chemistry on the performance of universal chimeric antigen receptor TCells for tumor killing. *Bioconjugate Chem*. 2020;31(7):1775–1783. doi:10.1021/acs.bioconjchem.0c00258.
17. Minutolo NG, Sharma P, Poussin M, Shaw LC, Brown DP, Hollander EE, Smole A, Rodriguez-Garcia A, Hui JZ, Zappala F. et al. Quantitative control of gene-engineered TCell activity through the covalent attachment of targeting ligands to a universal immune receptor. *J Am Chem Soc*. 2020;142(14):6554–6568. doi:10.1021/jacs.9b11622.
18. Lee YG, Marks I, Srinivasarao M, Kanduluru AK, Mahalingam SM, Liu X, Chu H, Low PS. Use of a single CAR T cell and several bispecific adapters facilitates eradication of multiple antigenically different solid tumors. *Cancer Res*. 2018;79(2):387–396. doi:10.1158/0008-5472.CAN-18-1834.
19. Bachmann M. The UniCAR system: a modular CAR T cell approach to improve the safety of CAR T cells. *Immunol Lett*. 2019;211:13–22. doi:10.1016/j.imlet.2019.05.003.
20. Zhang AQ, Hostetler A, Chen, LE, Mukkamala, V, Abraham, W, Padilla, LT, Wolff, AN, Maiorino, L, Backlund, CM, Aung, A, Melo, M. Universal redirection of CAR T cells against solid tumours via membrane-inserted ligands for the CAR. *Nat Biomed Eng*. 2023; 1–16. doi:10.1038/s41551-023-01048-8.
21. Vaughan TJ, Williams AJ, Pritchard K, Osbourn JK, Pope AR, Earnshaw JC, McCafferty J, Hodits RA, Wilton J, Johnson KS. et al. Human antibodies with sub-nanomolar affinities isolated from a large non-immunized phage display library. *Nat Biotechnol*. 1996;14(3):309–314. doi:10.1038/nbt0396-309.
22. Pfeifer A, Knigge U, Mortensen J, Oturai P, Berthelsen AK, Loft A, Binderup T, Rasmussen P, Elema D, Klausen TL. et al. Clinical PET of neuroendocrine tumors using 64Cu-dotatate: first-in-humans study. *J Nucl Med*. 2012;53(8):1207–1215. doi:10.2967/jnumed.111.101469.
23. Chan DL, Hayes AR, Karfis I, Conner A, Furtado O'Mahony L, Mileva M, Bernard E, Roach P, Marin G, Pavlakis N. et al. Dual [68Ga]DOTATATE and [18F]FDG PET/CT in patients with metastatic gastroenteropancreatic neuroendocrine neoplasms: a multicentre validation of the NETPET score. *Br J Cancer*. 2023;128(4):549–555. doi:10.1038/s41416-022-02061-5.
24. Camus B, Cottureau A-S, Palmieri L-J, Dermine S, Tenenbaum F, Brezault C, Coriat R. Indications of peptide receptor radionuclide therapy (PRRT) in Gastroenteropancreatic and pulmonary neuroendocrine tumors: an updated review. *J Clin Med*. 2021;10(6):1267. doi:10.3390/jcm10061267.
25. Boeckxstaens L, Pauwels E, Vandecaveye V, Deckers W, Cleeren F, Dekervel J, Vandamme T, Serdons K, Koole M, Bormans G. et al. Prospective comparison of [18F]AlF-nota-octreotide PET/MRI to [68Ga]Ga-dotatate PET/CT in neuroendocrine tumor patients. *EJNMMI Res*. 2023;13(1):53. doi:10.1186/s13550-023-01003-3.
26. Dude I, Zhang Z, Rousseau J, Hundal-Jabal N, Colpo N, Merkens H, Lin K-S, Bénard F. Evaluation of agonist and antagonist radioligands for somatostatin receptor imaging of breast cancer using positron emission tomography. *EJNMMI Radiopharm Chem*. 2017;2(1). doi:10.1186/s41181-017-0023-y.
27. Fani M, Braun F, Waser B, Beetschen K, Cescato R, Erchegyi J, Rivier JE, Weber WA, Maecke HR, Reubi JC. et al. Unexpected sensitivity of sst2 antagonists to N-Terminal radiometal modifications. *J Nucl Med*. 2012;53(9):1481–1489. doi:10.2967/jnumed.112.102764.
28. Millul J, Bassi G, Mock J, Elsayed A, Pellegrino C, Zana A, Dakhel Plaza S, Nadal L, Gloger A, Schmidt E. et al. An ultra-high-affinity small organic ligand of fibroblast activation protein for tumor-targeting applications. *Proc Natl Acad Sci*. 2021;118(16):e2101852118. doi:10.1073/pnas.2101852118.
29. Nixdorf D, Sponheimer M, Berghammer D, Engert F, Bader U, Philipp N, Kazerani M, Straub T, Rohrbacher L, Wange L. et al. Adapter CAR T cells to counteract T-cell exhaustion and enable flexible targeting in AML. *Leukemia*. 2023;37(6):1298–1310. doi:10.1038/s41375-023-01905-0.
30. Urbanska K, Lanitis E, Poussin M, Lynn RC, Gavin BP, Kelderman S, Yu J, Scholler N, Powell DJ. A universal strategy for adoptive immunotherapy of cancer through use of a novel T-cell antigen receptor. *Cancer Res*. 2012;72(7):1844–1852. doi:10.1158/0008-5472.CAN-11-3890.

31. Cho JH, Collins JJ, Wong WW. Universal chimeric antigen receptors for multiplexed and logical control of T cell responses. *Cell*. 2018;173(6):1426–1438.e11. doi:10.1016/j.cell.2018.03.038.
32. Bachmann D, Aliperta R, Bergmann R, Feldmann A, Koristka S, Arndt C, Loff S, Welzel P, Albert S, Kegler A. et al. Retargeting of UniCAR T cells with an in vivo synthesized target module directed against CD19 positive tumor cells. *Oncotarget*. 2017;9(7):7487–7500. doi:10.18632/oncotarget.23556.
33. Wallace MB, Meining A, Canto MI, Fockens P, Miehle S, Roesch T, Lightdale CJ, Pohl H, Carr-Locke D, Löhr M. et al. The safety of intravenous fluorescein for confocal laser endomicroscopy in the gastrointestinal tract. *Aliment Pharmacol Ther*. 2010;31(5):548–552. doi:10.1111/j.1365-2036.2009.04207.x.
34. Tamada K, Geng D, Sakoda Y, Bansal N, Srivastava R, Li Z, Davila E. Redirecting gene-modified T cells toward various cancer types using tagged antibodies. *Clin Cancer Res*. 2012;18(23):6436–6445. doi:10.1158/1078-0432.CCR-12-1449.
35. Lu Y, Xu L-C, Parker N, Westrick E, Reddy JA, Vetzl M, Low PS, Leamon CP. Preclinical pharmacokinetics, tissue distribution, and antitumor activity of a folate-hapten conjugate-targeted immunotherapy in hapten-immunized mice. *Mol Cancer Ther*. 2006;5(12):3258–3267. doi:10.1158/1535-7163.MCT-06-0439.
36. Vlashi E, Kelderhouse LE, Sturgis JE, Low PS. Effect of folate-targeted nanoparticle size on their rates of penetration into solid tumors. *ACS Nano*. 2013;7(10):8573–8582. doi:10.1021/nn402644g.
37. Cazzamalli S, Corso AD, Widmayer F, Neri D. Chemically defined antibody- and small molecule-drug conjugates for in vivo tumor targeting applications: a comparative analysis. *J Am Chem Soc*. 2018;140(5):1617–1621. doi:10.1021/jacs.7b13361.
38. Lee YG, Chu H, Lu Y, Leamon CP, Srinivasarao M, Putt KS, Low PS. Regulation of CAR T cell-mediated cytokine release syndrome-like toxicity using low molecular weight adapters. *Nat Commun*. 2019;10(1):2681. doi:10.1038/s41467-019-10565-7.
39. Arndt C, Loureiro LR, Feldmann A, Jureczek J, Bergmann R, Máthé D, Hegedüs N, Berndt N, Koristka S, Mitwasi N. et al. UniCAR T cell immunotherapy enables efficient elimination of radioresistant cancer cells. *OncoImmunology*. 2020;9(1):1743036. doi:10.1080/2162402X.2020.1743036.
40. Betts A, Haddish-Berhane N, Shah DK, van der Graaf PH, Barletta F, King L, Clark T, Kamperschroer C, Root A, Hooper A. et al. A translational quantitative systems pharmacology model for CD3 bispecific molecules: application to quantify T cell-mediated tumor cell killing by P-Cadherin LP DART®. *Aaps J*. 2019;21(4):66. doi:10.1208/s12248-019-0332-z.
41. Rader C. DARTs take aim at BiTEs. *Blood*. 2011;117(17):4403–4404. doi:10.1182/blood-2011-02-337691.
42. Chang ZL, Lorenzini MH, Chen X, Tran U, Bangayan NJ, Chen YY. Rewiring T-cell responses to soluble factors with chimeric antigen receptors. *Nat Chem Biol*. 2018;14(3):317–324. doi:10.1038/nchembio.2565.
43. Weckbecker G, Lewis I, Albert R, Schmid HA, Hoyer D, Bruns C. Opportunities in somatostatin research: biological, chemical and therapeutic aspects. *Nat Rev Drug Discov*. 2003;2(12):999–1017. doi:10.1038/nrd1255.
44. Reubi J, Waser B, Schaer J-C, Laissue JA. Somatostatin receptor sst1–sst5 expression in normal and neoplastic human tissues using receptor autoradiography with subtype-selective ligands. *Eur J Nucl Med*. 2001;28(7):836–846. doi:10.1007/s002590100541.
45. Kim JY, Kim J, Kim Y-I, Yang D-H, Yoo C, Park IJ, Ryoo B-Y, Ryu J-S, Hong S-M. Somatostatin receptor 2 (SSTR2) expression is associated with better clinical outcome and prognosis in rectal neuroendocrine tumors. *Sci Rep*. 2024;14(1):4047. doi:10.1038/s41598-024-54599-4.
46. Orlando C, Raggi CC, Bianchi S, Distanti V, Simi L, Vezzosi V, Gelmini S, Pinzani P, Smith MC, Buonamano A. et al. Measurement of somatostatin receptor subtype 2 mRNA in breast cancer and corresponding normal tissue. *Endocr Relat Cancer*. 2004;11(2):323–332. doi:10.1677/erc.0.0110323.
47. Myburgh R, Kiefer JD, Russkamp NF, Magnani CF, Nuñez N, Simonis A, Pfister S, Wilk CM, McHugh D, Friemel J. et al. Anti-human CD117 CAR T-cells efficiently eliminate healthy and malignant CD117-expressing hematopoietic cells. *Leukemia*. 2020;34(10):2688–2703. doi:10.1038/s41375-020-0818-9.
48. Fischer A, Kloos S, Maccio U, Friemel J, Remde H, Fassnacht M, Pamporaki C, Eisenhofer G, Timmers HJLM, Robledo M. et al. Metastatic pheochromocytoma and Paraganglioma: somatostatin receptor 2 expression, genetics, and therapeutic responses. *J Clin Endocrinol Metab*. 2023;108(10):2676–2685. doi:10.1210/clinem/dgad166.